Desalination and Water Treatment
www.deswater.com

doi: 10.5004/dwt.2017.20776

77 (2017) 221–228
May

Comparison of phosphorus removal characteristics using synthesized Fe-loaded granular composites

Linlin Ma, Nan Chen*, Chuanping Feng

School of Water Resources and Environment, China University of Geosciences, Beijing 100083, China, Tel. +86 10 82322281; Fax: +86 10 82321081; emails: chennan@cugb.edu.cn (N. Chen), cnjing2008@hotmail.com (L.L. Ma), fengcp@cugb.edu.cn (C.P. Feng)

Received 20 October 2016; Accepted 30 March 2017

ABSTRACT

This study evaluated the effectiveness of Fe-loaded granular composites (FGCs) for phosphorus removal from aqueous solution. Loess, montmorillonite, polymethyl methacrylate and $FeSO_4 \cdot 7H_2O$/$FeCl_2 \cdot 4H_2O$ were mixed to develop a new novel porous geological adsorbent by granulation procedure with the mass ratio of 3:4:1:2. Scanning electron microscope, Brunauer–Emmett–Teller, energy dispersive X-ray spectroscopy and X-ray diffraction were used to characterize the morphology and surface of synthesized samples. The FGC ($FeSO_4 \cdot 7H_2O$) was more effective for phosphorus adsorption than FGC ($FeCl_2 \cdot 4H_2O$) in adsorption capacity. The optimum pH for phosphorus removal on FGC ($FeSO_4 \cdot 7H_2O$) and FGC ($FeCl_2 \cdot 4H_2O$) was 7.0–9.0 and 6.0–7.0, respectively. The experimental data fitted reasonably well to Langmuir and Freundlich isotherm models for both of the geological adsorbents. The pseudo-first-order kinetic equation fitted well to FGC ($FeSO_4 \cdot 7H_2O$), while the pseudo-second-order kinetic equation fitted well to FGC ($FeCl_2 \cdot 4H_2O$). A chemical precipitation mechanism may be the predominant process for both adsorbents in this research. The practical application of FGCs on the effective removal of phosphorus from aqueous solution could be expected.

Keywords: Fe-loaded granular composite; Phosphorus; Adsorption isotherms; Kinetic studies

1. Introduction

Phosphorus is mainly as an essential nutrient for organisms in ecosystems. The geochemical behaviors of phosphorus were studied in the past few decades in various disciplines [1]. Phosphorus is involved in a wide variety of biological and chemical process in natural water and wastewater [2,3]. Amounts of soluble phosphorus in aqueous solution could cause severe ecological problems such as algal blooms and eutrophication [4]. In many countries, stringent regulations limit phosphorus level to be 0.05 mg/L to prevent increased algae growth [5]. Numerous studies concerning phosphorus removal from aqueous solution have been performed during recent years, such as adsorption, chemical precipitation, ion exchange, biological treatment and crystallization process [6–9]. Among these traditional methods, adsorption is one of the most popular separation and purification method due to its high selectivity, low operating cost, easy handling and effective removal efficiency. There are a large number of adsorbents have been studied for phosphorus removal, including alum and aluminum hydroxide, layered double hydroxides, dolomite, red mud, goethite, hybrid materials and collagen fiber [10–16]. However, most of them are still difficult to be applied because of high cost of reagent, short life expectancy or narrow pH ranges. In addition, most of these materials are powders, causing them to be difficult to separate from aqueous solution for reuse.

* Corresponding author.

Loess, an abundant natural geological material, originates from the western and northeast areas of China. Because of its cheapness and availability, it was used as base material in this experiment for Fe-loaded to adsorb phosphorous from contaminated water. Montmorillonite is a low cost and easily obtained mineral. Recently, some attempts have been carried out to be binder in the preparation process of ceramic materials. In order to keep the mechanical strength of adsorbent, montmorillonite was selected as the bonding material in this experiment. This study has developed a new type of adsorbent material (Fe-loaded granular composite [FGC]), which was characterized by specific surface areas and pore size distribution methods. These porous granular adsorbents were the solid phase of a spherical shape, with sufficient mechanical strength to retain its physical integrity after long-time adsorption process. Batch studies focused on comparing the phosphorus removal behaviors with two kinds of Fe-loaded ($FeSO_4{\cdot}7H_2O$/$FeCl_2{\cdot}4H_2O$) composites. It is necessary to figure out the removal behavior with different iron-loaded adsorption materials. Kinetic and isotherm experiments were conducted and different models were used to analyze the adsorption process of phosphorus at the solid–liquid interface, by describing the rate and mechanism of the adsorption process. The changes in surface morphology of FGCs before and after the adsorption reaction were also evaluated.

2. Materials and methods

2.1. Preparation of Fe-loaded granular composites

Loess (base material, particle size was <100 μm), a common, inexpensive deposit of eolian geological sedimentation, was collected in the garden of China University of Geosciences (Beijing). Montmorillonite (binder, particle size was <100 μm), polymethyl methacrylate (PMMA) (porogen, <20 μm), $FeSO_4{\cdot}7H_2O$ and $FeCl_2{\cdot}4H_2O$ were purchased from Sinopharm Chemical Reagent Co., Ltd., China. The FGCs were synthesized by the mixture (loess, montmorillonite, PMMA and $FeSO_4{\cdot}7H_2O$/$FeCl_2{\cdot}4H_2O$) with the mass ratio of 3:4:1:2. Ultrapure water (resistivity 18.2 MΩ cm at 25°C) was then added into the mixture to make a paste and the granulation procedure was conducted at room temperature (25°C ± 2°C) by manual [17]. Other chemical agents used were all analytical grade and all solutions were prepared with distilled water. The obtained granules were then dried at 105°C for 24 h and calcined at 600°C for 1 h in a muffle furnace. Finally, the prepared samples were cooled to room temperature and sealed in polythene bottle for further studies.

2.2. Batch adsorption experiments

A stock solution (100 mg/L) was prepared by dissolving 0.387 g anhydrous NaH_2PO_4 in 1 L of ultrapure water. All the solutions for phosphorus adsorption experiments and analysis were prepared by an appropriate dilution from the stock solution. The pH value for test solution was adjusted by 0.1 M HCl and NaOH. Batch adsorption experiments were carried out by adding 2 g of Fe-loaded adsorbent with 100 mL of phosphorus solution of desired concentrations at room temperature. Experimental variables were considered, such as: (a) contact time between granular adsorbent and phosphorus solution, 0–48 h; (b) adsorbent dosage, 5–25 g/L; (c) initial phosphorus concentration, 5–50 mg/L; (d) initial pH solution, 2.0–11.0 and (e) possible mechanisms for both of the different Fe-loaded adsorbents. Water samples were taken at the certain intervals and filtered through a 0.45 μm membrane filter to measure the residual phosphorus concentration. Each test was conducted in triplicate and averaged results were reported.

2.3. Characterization analysis

Phosphorus concentration was measured by the method of molybdenum antimony anti-spectrophotometer at 700 nm wavelength (DR-5000, Hach, USA) [18]. The surface morphology and spot elemental analysis of samples were carried out using the scanning electron microscope (SEM) and energy dispersive X-ray spectroscopy (EDS) detector (SSX-550, Shimadzu, Japan), respectively. The specific surface area of samples was determined by the Brunauer–Emmett–Teller (BET) method with N_2 adsorption (Coulter SA3100, Japan). Mineralogical phase characterization was carried out using quantitative X-ray diffraction (XRD; D8 Focus, Bruker, Germany). Solution pH was monitored with a standard pH meter (ORION 8157BNUMD, USA). The point of zero charge (pH_{pzc}) of FGCs was estimated using batch equilibrium techniques described by Chutia et al. [19].

3. Results and discussion

3.1. Influence of adsorbent dosage

The effect of adsorbent dosage for phosphorus removal by FGC ($FeSO_4{\cdot}7H_2O$) and FGC ($FeCl_2{\cdot}4H_2O$) was investigated with adsorbent dosage range from 5 to 25 g/L, initial pH 7.0 ± 0.1, initial phosphorus concentration of 10 mg/L and contact time of 36 h at 25°C. The results obtained are shown as adsorption percentage form in Fig. 1(a). It was observed that the adsorption percentage increased from 34.1% to 99.9% and 9.7% to 22.9% for FGC ($FeSO_4{\cdot}7H_2O$) and FGC ($FeCl_2{\cdot}4H_2O$) with an increase in adsorbent dosage from 5 to 25 g/L. However, after a dosage of 20 g/L, the amount removed per unit of adsorbent remained relatively stable. The increase in phosphorus removal with increase of adsorbent dosage is the consequence of a greater amount of available binding sites and energies for phosphorus. The distribution coefficient (K_D) for phosphorus on adsorbent was calculated by [20]:

$$K_D = [F^-]_{ads}/[F^-]_{diss}(1/C_p) \quad (1)$$

where C_p is the solid concentration in kg/L and K_D has the unit of L/kg. A distribution coefficient reflects the binding ability of the surface for an element.

The K_D value of a system mainly depends on the type of adsorbent surface and solution pH value. It was found that the K_D value increased with increase of adsorbent dosage for both of the FGC adsorbents (Fig. 1(b)). If the surface of adsorbent is homogeneous, the K_D value would not change with adsorbent dosage at a constant initial solution pH value. Therefore, the increased of K_D value (Fig. 1(b)) denoted the heterogeneous in nature of FGCs ($FeSO_4{\cdot}7H_2O$ and $FeCl_2{\cdot}4H_2O$) surface [21].

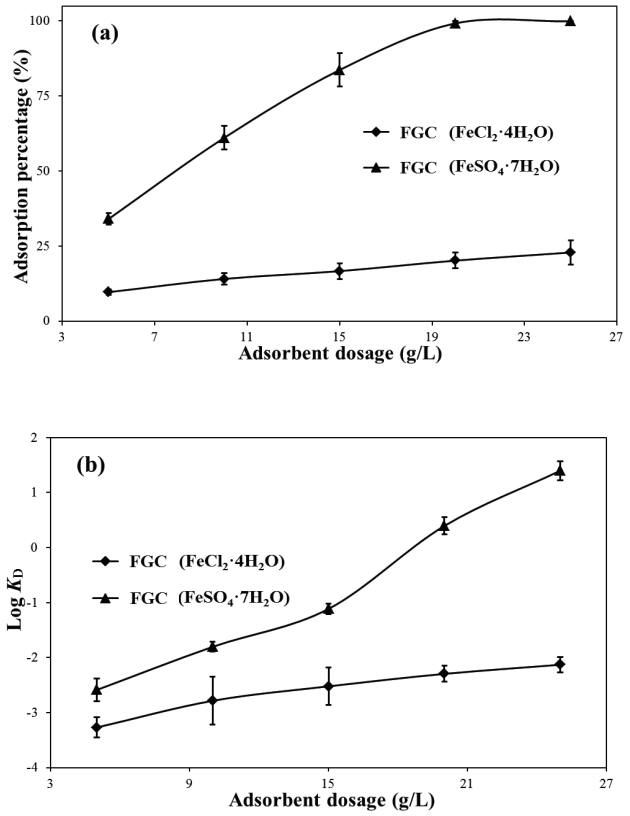

Fig. 1. (a) Effect of FGCs ($FeSO_4·7H_2O$ and $FeCl_2·4H_2O$) dosage variation for phosphorus removal (initial pH 7.0 ± 0.1, initial phosphorus concentration 10 mg/L, contact time 36 h and temperature 25°C ± 1°C). (b) The plot of $\log K_D$ value as a function of FGCs ($FeSO_4·7H_2O$ and $FeCl_2·4H_2O$) dosage (data corresponding to (a)).

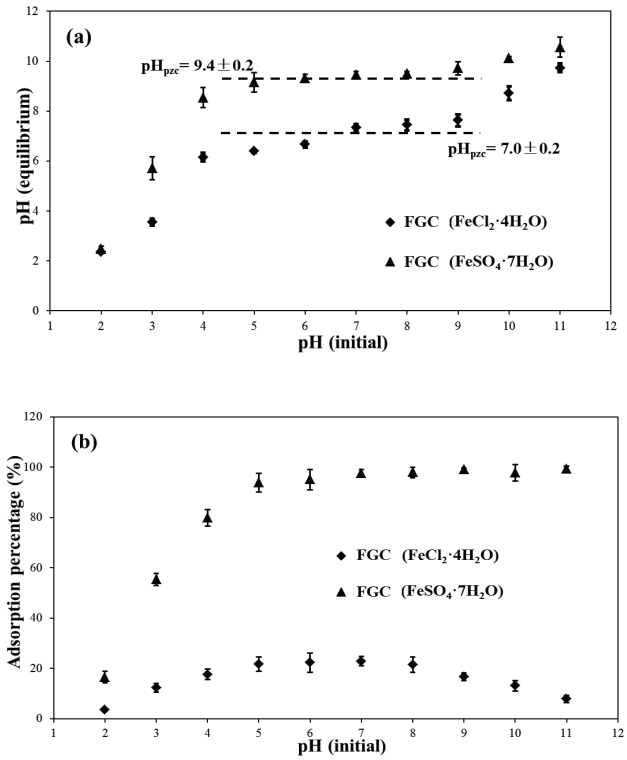

Fig. 2. (a) pH_{pzc} of FGCs ($FeSO_4·7H_2O$ and $FeCl_2·4H_2O$). (b) Effect of pH on phosphorus removal by FGCs ($FeSO_4·7H_2O$ and $FeCl_2·4H_2O$) (adsorbent dosage 20 g/L, contact time 36 h, initial pH 2.0–11.0, initial phosphorus concentration 10 mg/L and temperature 25°C ± 1°C).

3.2. Determination of pH_{pzc} and influence of pH

The pH value of solution where the net surface charge of adsorbent is zero is defined as pH_{pzc}. As shown in Fig. 2(a), a plot of pH values of filtered solution after equilibrium (pH_{final}) as a function of initial pH values ($pH_{initial}$) provides pH_{pzc} of the adsorbents by the common plateau of constant pH to the ordinate at 9.4 ± 0.2 and 7.0 ± 0.2 for FGC ($FeSO_4·7H_2O$) and FGC ($FeCl_2·4H_2O$), respectively. After the calcination process, the ferrous ion in $FeSO_4·7H_2O$ and $FeCl_2·4H_2O$ changed to be iron oxides and the content of Fe element in FGC ($FeSO_4·7H_2O$) is around 2.5 times than FGC ($FeCl_2·4H_2O$) (shown in Table 1). Therefore, the FGC ($FeSO_4·7H_2O$) performed a better phosphorus adsorption capacity than the FGC ($FeCl_2·4H_2O$), and hence increased the value of pH_{pzc} with the phosphorus concentration decreased in aqueous solution.

It has been reported that adsorption of anionic substances from aqueous medium depends heavily on the protonation pH range in liquid environment [22]. Influence of solution pH for phosphorus removal by FGC ($FeSO_4·7H_2O$) and FGC ($FeCl_2·4H_2O$) was carried out with solution pH ranging from 2.0 to 11.0 and the results are shown in Fig. 2(b). It is evident that for FGC ($FeSO_4·7H_2O$) sample, the maxima occurs at pH range of 7.0–9.0, with a maximum adsorption percentage of 99.1%. Whereas for FGC ($FeCl_2·4H_2O$) sample, the maxima is in the pH range of 6.0–7.0, with a removal adsorption percentage of 22.9%. The adsorption process by FGC ($FeSO_4·7H_2O$) was more favored in neutral or partial alkaline (7.0–9.0) solution, while FGC ($FeCl_2·4H_2O$) was more favored in neutral (6.0–7.0) solution. It can be explained by the pH_{pzc} value (9.4 ± 0.2 and 7.0 ± 0.2) of these two synthesized geological materials. The phosphorus adsorption mechanism may be attributed to the electrostatic attraction and chemical precipitation interactions between the iron oxides on the surface of FGCs. At acidic conditions (pH < 4), $H_2PO_4^-$ and HPO_4^{2-} ions may have a weak combining ability with the iron compounds on the surface of FGCs. A chemical precipitation mechanism may be the predominant process at pH > 7.0 in aqueous solution. While, the surface of FGCs is negative at alkaline conditions (pH > 9), which may decrease the electrostatic attraction with PO_4^{3-} ions. This results were found to be similar to that had been reported for phosphorus adsorption by Chen et al. [17].

3.3. Equilibrium isotherms

The adsorption equilibrium isotherm models would help to reveal the adsorption mechanism, the surface properties and affinity of the adsorbent. In the current study, the Langmuir and Freundlich isotherm models were used to describe the dynamic balance on solid (FGC adsorbents) and liquid (dissolved phosphorus) interface.

Table 1
Langmuir and Freundlich isotherm parameters for the adsorption on FGCs at initial pH 7.0 ± 0.1, initial phosphorus concentration 5–50 mg/L, contact time 36 h, adsorbent dosage 20 g/L and temperature 25°C ± 1°C

Granular adsorbent	Langmuir isotherm			Freundlich isotherm		
	q_m (mg/g)	B (L/mg)	R^2	K_f (mg/g)	n	R^2
FGC ($FeSO_4·7H_2O$)	1.4255	0.0650	0.9856	0.3064	3.3456	0.9321
FGC ($FeCl_2·4H_2O$)	0.3930	0.0546	0.9994	0.0352	1.8067	0.9643

The Langmuir isotherm model is based on the hypothesis that uptake or adsorption occurs on a homogenous surface by monolayer adsorption without interaction between adsorbed molecule, and is expressed as [23]:

$$q_e = q_m B C_e / (1 + B C_e) \quad (2)$$

where q_m represents the maximum adsorption capacity (mg/g) and B is a constant related to affinity and energy of binding sites (L/mg).

The Freundlich isotherm model assumes a monolayer adsorption process with a heterogeneous energetic distribution of active sites and with interaction between adsorbed molecules. It is expressed mathematically as [24]:

$$q_e = K_f C_e^{1/n} \quad (3)$$

where K_f and n are the Freundlich coefficients. K_f provides an indication of the adsorption capacity (mg/g) and n is related to the intensity of adsorption.

Fig. 3 demonstrates the plot of C_e vs. q_e on the adsorption of phosphorus by FGC ($FeSO_4·7H_2O$) and FGC ($FeCl_2·4H_2O$). The equilibrium data of Fig. 3 have been analyzed by non-linear regression method using the isotherm Eqs. (2) and (3). Table 1 shows the estimated model parameters. It was found that the adsorption data for phosphorus removal by FGCs ($FeSO_4·7H_2O$/$FeCl_2·4H_2O$) were fitted well to both Langmuir and Freundlich isotherm models. The magnitude of the Langmuir constant B has small values (0.0650 and 0.0546 L/mg), which denoted a low heat of adsorption. The Freundlich constant n values (3.3456 and 1.8067) illustrated the high bond strength between solid and liquid interface and it also indicates the adsorbent surface to be heterogeneous, which is in accordance with the results in section 3.1.

3.4. Kinetic studies

In order to investigate the adsorption rate constants of phosphorus on FGCs ($FeSO_4·7H_2O$/$FeCl_2·4H_2O$), the pseudo-first-order and pseudo-second-order models were employed. The model equations are presented as follows [25,26]:

$$\log(q_e - q_t) = \log q_e - k_1 t / 2.303 \quad (4)$$

$$t / q_t = 1 / (k_2 q_e^2) + t / q_e \quad (5)$$

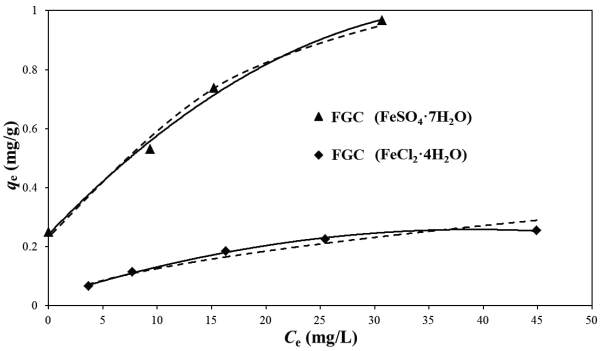

Fig. 3. The plot of C_e vs. q_e on phosphorus adsorption by FGCs ($FeSO_4·7H_2O$ and $FeCl_2·4H_2O$) (__ Langmuir isotherm; _ _ _ Freundlich isotherm) (initial pH 7.0 ± 0.1, adsorbent dosage 20 g/L, contact time 36 h and temperature 25°C ± 1°C).

where q_t and q_e are the amount of adsorbed phosphorus (mg/g) at time t and at equilibrium time (h), respectively. k_1 (1/h) and k_2 (g/(mg·h)) are first-order and second-order rate constants for adsorption.

The kinetic parameters estimated from Eqs. (4) and (5) are shown in Table 2. According to the values of correlation coefficient, it was found that the pseudo-first-order equation (R^2 = 0.9754) fitted better than the pseudo-second-order equation (R^2 = 0.9416) for FGC ($FeSO_4·7H_2O$). On the contrary, the pseudo-second-order equation (R^2 = 0.9670) described more appropriate than the pseudo-first-order equation (R^2 = 0.9176) for FGC ($FeCl_2·4H_2O$). The calculated q_e values obtained from pseudo-first-order and pseudo-second-order equations were also found close to the experimental q_e for FGC ($FeSO_4·7H_2O$) and FGC ($FeCl_2·4H_2O$), respectively. Thus, it had been concluded that the adsorption process obeyed the pseudo-first-order and pseudo-second-order kinetic model for synthesized FGC ($FeSO_4·7H_2O$) and FGC ($FeCl_2·4H_2O$), respectively. The adsorption rate constant was found to be 0.1145 and 0.3210 g/(mg·h) for FGC ($FeSO_4·7H_2O$) and FGC ($FeCl_2·4H_2O$), respectively.

Besides adsorption at the outer surface of the adsorbent, the dihydrogen phosphate ion and phosphate ion may also diffuse into the interior of the porous geological adsorbent [27]. Therefore, it is important to investigate the rate determining step in phosphorus adsorption process by using the intra-particle diffusion equation [28]:

$$q_t = k_p t^{0.5} \quad (6)$$

where q_t is the amount adsorbed (mg/g) at a given time t (h), k_p (mg/g $h^{0.5}$) is the intra-particle diffusion rate constant.

Table 2
Kinetic constants for adsorption of phosphorus on FGCs at initial pH 7.0 ± 0.1, initial phosphorus concentration 10 mg/L, adsorbent dosage 20 g/L and temperature 25°C ± 1°C

Granular adsorbent	$q_{e,exp}$ (mg/g)	Pseudo-first-order			Pseudo-second-order		
		k_1 (1/h)	$q_{e,cal}$ (mg/g)	R^2	k_2 [g/(mg·h)]	$q_{e,cal}$ (mg/g)	R^2
FGC ($FeSO_4·7H_2O$)	0.4995	0.1154	0.7468	0.9754	0.0549	0.8280	0.9416
FGC ($FeCl_2·4H_2O$)	0.1145	1.8104	0.8997	0.9176	0.3210	0.1709	0.9670

Note: $q_{e,exp}$ and $q_{e,cal}$ represent the measured value and predicted by kinetic models value of solid phase phosphorus concentrations at equilibrium.

Fig. 4 shows the value of q_t vs. the square root of t. It is observed that the intra-particle diffusion model of phosphorus adsorption on FGC ($FeSO_4·7H_2O$) and FGC ($FeCl_2·4H_2O$) both are not linear forms over the whole time range. The adsorption process can be divided into three stages: first, transport of phosphorus to the external surface of the adsorbent from bulk solution across the boundary layer surrounding the adsorbent particle (external mass transfer); second, adsorption of phosphorus onto particle surface, which always happens very fast; finally, exchange of the adsorbed phosphorus with the structural metal elements (iron) of adsorbent particles, or diffusion of phosphorus in the internal surface of porous geological materials (intra-particle diffusion). In addition, the linear portions did not pass the origin in Fig. 4, which indicated that mechanisms of phosphorus removal by FGC ($FeSO_4·7H_2O$) and FGC ($FeCl_2·4H_2O$) were complex, and the intra-particle diffusion was not the only determining step. Similar results have been reported for phosphorus adsorption on Aleppo pine and hydrous niobium oxide [29].

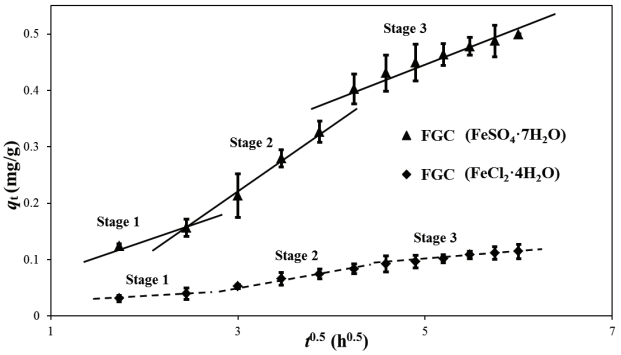

Fig. 4. Intra-particle diffusion modeling of phosphorus adsorption on FGCs ($FeSO_4·7H_2O$ and $FeCl_2·4H_2O$) (initial pH 7.0 ± 0.1, initial phosphorus concentration 10 mg/L, adsorbent dosage 20 g/L, contact time 36 h and temperature 25°C ± 1°C).

3.5. Possible mechanisms

It is known that certain anions (dihydrogen phosphate, hydrogen phosphate, phosphate, etc.) that are strongly adsorbed on metal hydroxides through the ligand exchange (inner sphere or outer sphere complex). In the present study, the metal hydroxide is mainly the iron hydroxide. An inner sphere complex is formed when the adsorbed ligand is directly linked to the metal ion by covalent bonding, and an outer complex, which involves electrostatic bonding, is formed when a water molecule is retained between the exchange site and the adsorbed ligand [30]. Accordingly, it can be assumed that the phosphorus adsorption on FGCs may be due to the following reactions:

$$FeSO_4 \times 7H_2O/FeCl_2 \times 4H_2O + O_2 \rightarrow \equiv SO/\equiv ClO + Fe_2O_3 + H_2O \quad (7)$$

$$Fe_2O_3 + H_2O \rightarrow \equiv Fe - OH \quad (8)$$

$$\equiv Fe - OH + H^+ + H_2PO_4^- \rightarrow \equiv Fe - OH_2^+ + H_2PO_4^- \quad (9)$$

$$\equiv Fe - OH + 2H^+ + HPO_4^{2-} \leftrightarrow \equiv Fe - OH^{2+}HPO_4^{2-} + H^+ \quad (10)$$

$$\equiv Fe - OH + 3H^+ + PO_4^{3-} \leftrightarrow \equiv Fe - OH_2^+ + PO_4^{3-} + 2H^+ \quad (11)$$

where –OH is a hydroxyl group, and $–H_2PO_4^-$, HPO_4^{2-} and PO_4^{3-} are the adsorbed ligands at corresponding pH values.

In the present study, phosphorus adsorption behaviors were performed by comparing with FGC ($FeSO_4·7H_2O$) and FGC ($FeCl_2·4H_2O$), and the results are of the horizon of otherness. The samples of FGC ($FeSO_4·7H_2O$) and FGC ($FeCl_2·4H_2O$) were red-colored and claret-colored particles, respectively, and with diameters of 2–3 mm (Figs. 5(a) and (b)). The Vickers hardness of FGC ($FeSO_4·7H_2O$) and FGC ($FeCl_2·4H_2O$) ceramic particles was 98.8 and 97.4 kg/mm^2, respectively, which indicates the stability and firmness of the adsorbents. The EDS (Table 3) showed the atom proportion of Fe at the surface was around 2.5 times in FGC ($FeSO_4·7H_2O$) than in FGC ($FeCl_2·4H_2O$) adsorbent. According to the assumed mechanisms, phosphorus was mainly bound with the iron oxide and its hydrate hydroxide, therefore, the content of iron oxide is an important parameter for the performance of phosphorus adsorption. The surface morphology of FGC ($FeSO_4·7H_2O$) and FGC ($FeCl_2·4H_2O$) was shown in Figs. 5(c) and (d). Compared with FGC ($FeCl_2·4H_2O$), FGC ($FeSO_4·7H_2O$) had a significantly rougher surface with a lot of pore structures (Fig. 5(c)). Conversely, the relatively smooth surface of FGC ($FeCl_2·4H_2O$) appeared to be less porosity which would make phosphorus difficult to attach to the adsorbent (Fig. 5(d)). In addition, from the results of XRD pattern in Fig. 6, it can be seen that hematite/gamma-hematite was the predominant iron mineral in the pristine FGC ($FeSO_4·7H_2O$), while iron-oxide-beta hematite and wustite were the predominant iron minerals in the pristine FGC ($FeCl_2·4H_2O$). According to the results obtained from the

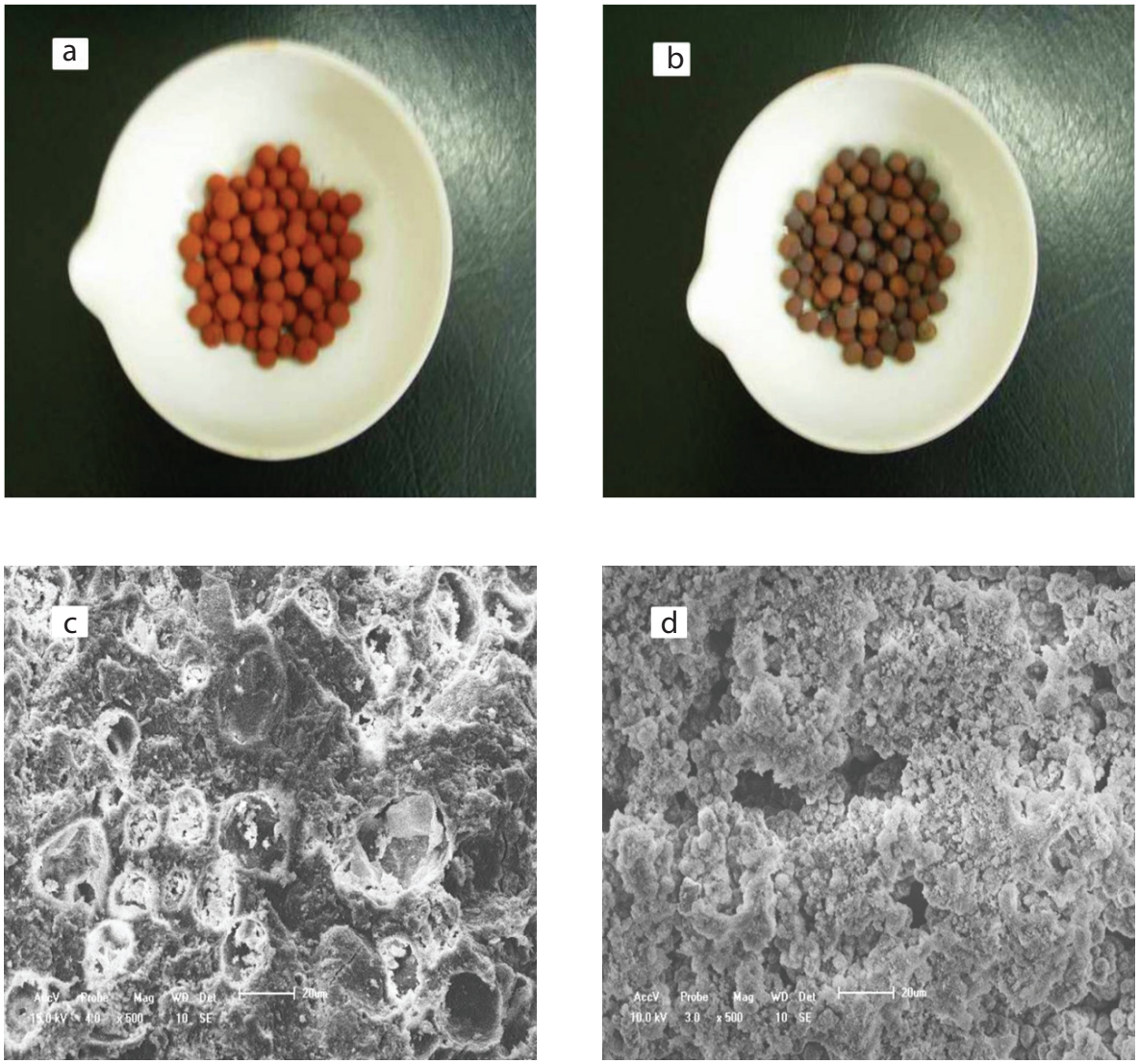

Fig. 5. Photos of pristine: (A) FGC ($FeSO_4 \cdot 7H_2O$) and (B) FGC ($FeCl_2 \cdot 4H_2O$); SEM images of pristine: (C) FGC ($FeSO_4 \cdot 7H_2O$) 1,000× and (D) FGC ($FeCl_2 \cdot 4H_2O$) 1,000×.

Table 3
Chemical analysis and surface area characterization of each mineral sample and Fe-loaded porous granular composite (FGC)

Analysis of each clay sample and FGCs by SEM–EDS test							
Composition (wt%)	O	Si	Fe	Al	Ca	Mg	pH_{pzc}
Loess	75.79	10.45	1.20	5.15	5.86	1.55	–
Montmorillonite	65.86	21.17	0.10	9.58	0.76	2.53	–
FGC ($FeSO_4 \cdot 7H_2O$)	57.14	11.92	22.43	5.74	1.33	1.44	9.4 ± 0.2
FGC ($FeCl_2 \cdot 4H_2O$)	64.63	16.44	9.94	6.83	1.00	1.16	7.0 ± 0.2

Surface area and pore volume analysis by BET test				
	BET surface area (m^2/g)	*T*-plot surface area (m^2/g)	Average pore diameter (nm)	Pore volume (cm^3/g)
FGC ($FeSO_4 \cdot 7H_2O$)	25.54	18.20	11.23	0.1803
FGC ($FeCl_2 \cdot 4H_2O$)	9.86	6.52	5.07	0.0827

Note: The effect on LOI (600°C) has been neglected.

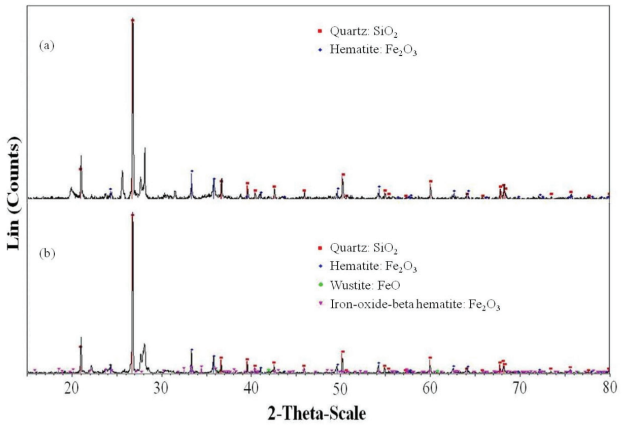

Fig. 6. XRD patterns of the pristine: (a) FGC ($FeSO_4 \cdot 7H_2O$) and (b) FGC ($FeCl_2 \cdot 4H_2O$).

batch experiments, it can be revealed that the hematite (especially gamma-hematite) mineral may have a better affinity with phosphorus than the iron-oxide-beta hematite and wustite minerals, while the specific mechanism in detail should be tested and verified in further research.

4. Conclusion

Results obtained from this study have provided some valuable information regarding the characteristics and mechanisms of phosphorus removal by Fe-loaded porous granular composites. FGC ($FeSO_4 \cdot 7H_2O$) and FGC ($FeCl_2 \cdot 4H_2O$) were both used for phosphorus removal from aqueous solution. FGC ($FeSO_4 \cdot 7H_2O$) was more effective and applicable for phosphorus removal than FGC ($FeCl_2 \cdot 4H_2O$). Maximum adsorption efficiency by FGC ($FeSO_4 \cdot 7H_2O$) and FGC ($FeCl_2 \cdot 4H_2O$) at pH 7.0–9.0 and 6.0–7.0 were 99.1% and 22.9%, respectively. The equilibrium data fitted well to both Langmuir and Freundlich isotherm models for two kinds of the FGCs ($FeSO_4 \cdot 7H_2O$/$FeCl_2 \cdot 4H_2O$). In addition, the pseudo-first-order equation fitted well to FGC ($FeSO_4 \cdot 7H_2O$), while the pseudo-second-order equation fitted well to FGC ($FeCl_2 \cdot 4H_2O$). Intra-particle diffusion model played an important role in adsorption process for both of the FGC ($FeSO_4 \cdot 7H_2O$) and FGC ($FeCl_2 \cdot 4H_2O$). The adsorption mechanisms for Fe-loaded porous geological materials were also investigated and assumed. In summary, the $FeSO_4 \cdot 7H_2O$ loaded porous granular composite is a potential adsorbent, which may be used in practical application for phosphorus removal from aqueous solution in the future.

Acknowledgment

The authors thank the National Natural Science Foundation (NSFC) (21407129) and the Fundamental Research Funds for the Central Universities (2652016032) for financial support for this work.

References

[1] S. Benyoucef, M. Amrani, Adsorption of phosphate ions onto low cost Aleppo pine adsorbent, Desalination, 275 (2011) 231–236.
[2] R. Chitrakar, R. Tezuka, A. Sonoda, K. Sakane, K. Ooi, T. Hirotsu, Selective adsorption of phosphate from seawater and wastewater by amorphous zirconium hydroxide, J. Colloid Interface Sci., 297 (2006) 426–433.
[3] L. Borgninoa, M.J. Avenab, C.P. De Pauli, Synthesis and characterization of Fe(III)-montmorillonites for phosphate adsorption, Colloids Surf., A, 341 (2009) 46–52.
[4] L.J. Puckett, Identifying the major sources of nutrient water pollution, Environ. Sci. Technol., 29 (1995) 408A–414A.
[5] H. Behrendt, D. Opitz, M. Klein, Arch. Nat. Conserv. Landscape Res., 35 (1997) 329.
[6] S. Asaoka, T. Yamamoto, Characteristics of phosphate adsorption onto granulated coal ash in seawater, Mar. Pollut. Bull., 60 (2010) 1188–1192.
[7] R.G. Penetra, M.A.P. Reali, E. Foresti, J.R. Campos, Post-treatment of effluents from anaerobic reactor treating domestic sewage by dissolved-air flotation, Water Sci. Technol., 40 (1999) 137–143.
[8] A. Gieseke, P. Arnz, R. Amann, A. Schramm, Simultaneous P and N removal in a sequencing batch biofilm reactor: insights from reactor and microscale investigations, Water Res., 36 (2002) 501–509.
[9] E. Eggers, A.H. Dirkzwager, H.V.D. Honing, Full-scale experiences with phosphate crystallization in a crystalactor, Water Sci. Technol., 24 (1991) 333–334.
[10] D.A. Georgantas, H.P. Grigoropoulou, Orthophosphate and metaphosphate ion removal from aqueous solution using alum and aluminum hydroxide, J. Colloid Interface Sci., 315 (2007) 70–79.
[11] J. Das, B.S. Patra, N. Baliarsingh, K.M. Parida, Adsorption of phosphate by layered double hydroxides in aqueous solution, Appl. Clay Sci., 32 (2006) 252–260.
[12] S. Karaca, A. Gurses, M. Ejder, M. Acikyildiz, Kinetic modeling of liquid-phase adsorption of phosphate on dolomite, J. Colloid Interface Sci., 277 (2004) 257–263.
[13] J. Pradhan. J. Das, S. Das, R.S. Thakur, Adsorption of phosphate from aqueous solution using activated red mud, J. Colloid Interface Sci., 204 (1998) 169–172.
[14] B. Nowack, A.T. Stone, Competitive adsorption of phosphate and phosphonates onto goethite, Water Res., 40 (2006) 2201–2209.
[15] L.M. Blaney, S. Cinar, A.K. Sengupta, Hybrid anion exchanger for trace phosphate removal from water and wastewater, Water Res., 41 (2007) 1603–1613.
[16] X.P. Liao, Y. Ding, B. Wang, B. Shi, Adsorption behavior of phosphate on metal-ions-loaded collagen fiber, Ind. Eng. Chem. Res., 45 (2006) 3896–3901.
[17] N. Chen, Z.Y. Zhang, C.P. Feng, M. Li, D.R. Zhu, R.Z. Chen, N. Sugiura, An excellent fluoride sorption behavior of ceramic adsorbent, J. Hazard Mater., 183 (2010) 460–465.
[18] Water and Wastewater Monitoring Analysis Method, 4th ed., China Environmental Science Press, 2002, pp. 246–248.
[19] P. Chutia, S. Kato, T. Kojima, S. Satokawa, Arsenic adsorption from aqueous solution on synthetic zeolites, J. Hazard. Mater., 162 (2009) 440–447.
[20] J.W. Murray, W. Stumm, Eds., Aquatic Surface Chemistry: Chemical Processes at the Particle-Water Interface, Vol. 52, John Wiley & Sons, New York, 1988, p. 1742.
[21] M.G. Sujana, S. Anand, Iron and aluminum based mixed hydroxides: a novel sorbent for fluoride removal from aqueous solutions, Appl. Surf. Sci., 256 (2010) 6956–6962.
[22] I.D. Smiciklas, S.K. Milonjic, P. Pfendt, S. Raicevic, The point of zero charge and sorption of cadmium (II) and strontium (II) ions on synthetic hydroxyapatite, Sep. Purif. Technol., 18 (2000) 185–194.
[23] I. Langmuir, The constitution and fundamental properties of solids and liquids, J. Am. Chem. Soc., 38 (1916) 2221–2295.
[24] H.M.F. Freundlich, Über die adsorption in losungen, Z. Phys. Chem., 57A (1906) 385–470.
[25] S. Lagergren, K. Svenska, About the theory of so called adsorption of soluble substances, K. Sven. Vetensk.akad. Handl., 24 (1898) 1–39.

[26] Y.S. Ho, G. Mckay, Pseudo-second order model for sorption process, Process Biochem., 34 (1999) 451–465.
[27] M. Mahramanlioglu, I. Kizilcikli, I.O. Bicer, Adsorption of fluoride from aqueous solution by acid treated spent bleaching earth, J. Fluorine Chem., 115 (2002) 41–47.
[28] W.J. Weber Jr., J.C. Morris, Kinetics of adsorption on carbon from solution, J. Sanit. Eng. Div. ASCE, 89 (1963) 31–59.
[29] L.A. Rodrigues, M.L.C. Pinto da Silva, Thermodynamic and kinetic investigations of phosphate adsorption onto hydrous niobium oxide prepared by homogeneous solution method, Desalination, 263 (2010) 29–35.
[30] S. Ouvrard, Ph. de Donato, M.O. Simonnot, S. Begin, J. Ghanbaja, M. Alnot, Y.B. Duval, F. Lhote, O. Barres, M. Sardin, Natural manganese oxide: combined analytical approach for solid characterization and arsenic retention, Geochim. Cosmochim. Acta, 69 (2005) 2715–2724.